Photophysics and Crystal Structure of a Europium(III) Cryptate Incorporating 3,3′-Biisoquinoline-2,2′-dioxide

P. Gawryszewska,[†] L. Jerzykiewicz,[†] M. Pietraszkiewicz,[‡] J. Legendziewicz,*[,†] and J. P. Riehl*[,§]

Faculty of Chemistry, University of Wroclaw, 14 F. Joliot-Curie Str., 50-383 Wroclaw, Poland, Institute of Physical Chemistry, Polish Academy of Sciences, Kasprzaka 42, 01-224 Warszawa, Poland, and Department of Chemistry, University of Minnesota, Duluth, Duluth, Minnesota 55812

Received April 28, 2000

Increased interest in the emission properties of lanthanide(III) (Eu and Tb) complexes containing ultraviolet and visible sensitizers is being driven by the desire to produce efficient and selective luminescent probes of biological structure. Of special interest are cryptates and other macrocyclic chelating ligands that efficiently encapsulate the lanthanide ions. These species also form relatively stable systems and in some cases are well protected from penetration of the first coordination sphere by solvent molecules and counterions. This work describes the X-ray structure and various spectroscopic measurements on a europium cryptate containing 3,3′-biisoquinoline-2,2′-dioxide ($biqO_2$). This cryptate has been previously recognized for special stability and luminescence efficiency. The compound, $(Eu:biqO_2.2.2)(CF_3SO_3)_3{\cdot}CH_3CN{\cdot}H_2O$, forms rhombic crystals with the space group *Pbca*. Absorption, emission, and excitation spectra at 293, 77, and 4 K as well as luminescence decay time measurements are used to characterize the solid state and solutions. The ligand-to-metal energy-transfer mechanism and thermally activated back-energy-transfer processes are analyzed and compared to previously published results on related Eu(III) cryptate systems. Preliminary results on the use of high liquid pressure to perturb ligand singlet and triplet states and, as a consequence, probe the ligand−metal orbital interactions are also presented.

1. Introduction

Complexes containing one of the several luminescent lanthanide(III) ions are being increasingly used as highly sensitive and selective fluoroimmunoassay agents.[1−5] The continued development and refinement of these agents relies upon the ability to construct complexes that meet fairly rigorous requirements of stability in aqueous media containing relatively large concentrations of competing cations, high-luminescence intensity, and accessible chemistry to design an overall structure that is highly selective to the system of interest. Much of the progress in this area has employed the so-called bifunctional approach in which the design and synthesis of a stable luminescent lanthanide species is considered somewhat separately from the biological selectivity and sensitivity. Commercial fluoroimmunoassays involving luminescent lanthanide-(III) ions, in fact, involve two separate species: one which is designed to bind in a highly specific manner, and then a second complex which is produced and may be detected by luminescence.[6] Much effort is being devoted to the design of new luminescent lanthanide complexes suitable as fluoroimmunoassay agents, which both have the potential to bind selectively and are strongly luminescent.

The most emissive lanthanide(III) ions are Tb(III) and Eu(III). These ions emit in the visible region of the spectrum, far removed from most intrinsic fluorescence of organic or biological molecules. If overlapping luminescence is present, it is usually the case that it can be easily separated from the lanthanide luminescence by simple time discrimination, because the lifetimes of Eu(III) and Tb(III) are normally on the order of 0.1−2 ms. This is, of course, much longer than the luminescence from most organic luminophores. The structural requirements for a lanthanide complex to be strongly luminescent are different than those associated with effective lanthanide-based magnetic resonance imaging contrast agents, such as the complex of Gd(III) with DTPA (diethylenetriaminepentaacetic acid).[7] In both situations, one needs to have a complex with a very high stability constant, but in the latter case, one also requires the availability of coordination sites for solvent water molecules that can be affected by the spin center. It is important in designing luminescent species involving lanthanide(III) ions that the solvent be effectively eliminated from the first coordination sphere, because this often presents a competitive nonradiative relaxation pathway. Another primary requirement is that the ligand contains a strongly absorbing transition that will populate the emitting state of the lanthanide ion through radiationless energy transfer, because direct excitation of intraconfigurational f ↔ f transitions is very weak.

The various requirements associated with complex stability and luminescence efficiency have led to a number of studies involving lanthanide complexes with macrocyclic ligands containing heteroaromatic species.[8−12] Of special interest to this

[†] University of Wroclaw.
[‡] Polish Academy of Sciences.
[§] University of Minnesota, Duluth.

(1) Clark, I. D.; Macmanus, J. P.; Szabo, A. G. *Clin. Biochem.* **1995**, *28*, 131−135.
(2) Kurskainen, P.; Dahlen, P.; Ylikoski, J.; Kwiatkowski, M.; Siitari, H.; Lovgren, T. *Nucleic Acids Res.* **1991**, *19*, 1057−1061.
(3) Morton, R. C.; Diamandis, E. P. *Anal. Chem.* **1990**, *62*, 1841.
(4) Takalo, H.; Mikkala, V.-M.; Merio, L.; Rodriguez-Ubis, J. C.; Sedana, S.; Juanes, O.; Brunet, E. *Helv. Chim. Acta* **1997**, *80*, 372−387.
(5) Li, M.; Selvin, P. R. *Bioconjugate Chem.* **1997**, *8*, 127−132.
(6) Diamandis, E. P.; Christopoulos, T. K. *Anal. Chem.* **1990**, *62*, 1149.
(7) Hall, J.; Haner, R.; Aime, S.; Botta, M.; Faulkner, S.; Parker, D.; De Sousa, A. S. *New J. Chem.* **1998**, 627.
(8) Alpha, B.; Lehn, J.-M.; Matkis, G. *Angew. Chem.* **1987**, *99*, 259.

10.1021/ic0004683 CCC: $19.00
Published on Web 10/25/2000

research effort are ligands containing aromatic *N*-oxide functional groups.[11,12] It is well-known that ligands containing these groups are often very stable, and energy transfer from the aromatic $\pi\pi^*$ excited states, that are excited in the ultraviolet, to the lanthanide(III) ion may be very efficient. One approach to the design of this type of species is the encapsulation of the luminescent lanthanide ion in a cryptate incorporating a heteroaromatic *N*-oxide unit. Very recently we have reported the results of preliminary spectroscopic investigations on several different types of such lanthanide cryptates in solution, in the solid state, and prepared in sol gels.[13] In the present work, we present a detailed study of a europium cryptate containing 3,3′-biisoquinoline-2,2′-dioxide ($biqO_2$) for the purpose of probing the specific energetic and structural characteristics that influence luminescence efficiency. This cryptate has already been shown to have exceptional stability and luminescence efficiency, and it is an excellent model species for the detailed structural and spectroscopic analysis necessary to develop a better understanding of the energetics and dynamics of this class of molecules. Included in the work presented here is the X-ray crystal structure data for this europium cryptate. This represents one of the very few structures of this type that have appeared in the literature. Spectroscopic results are presented and discussed for the solid Eu(III) cryptate as well as for solutions of the Eu(III) cryptate dissolved in H_2O, D_2O, and CH_3CN. Spectroscopic measurements covering a wide range of temperatures from 4 to 300 K will be reported. We also report luminescence results as a function of liquid pressure. Of special interest in this work is the relative contribution of the radiative and nonradiative paths to excited-state deactivation. These will be discussed along with implications concerning future initiatives to design efficient fluoroimmunoassay agents.

2. Experimental Section

A cryptand (denoted $biqO_2.2.2$) incorporating ″$biqO_2$ and a complex of this cryptand with Eu(III) were prepared according to previously published procedures.[14,15] Triflate ($CF_3SO_3^-$) was employed as the

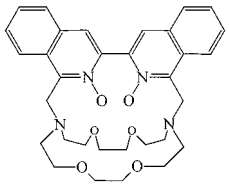

$biqO_2.2.2$

counterion. The final complex has the formula $(Eu:biqO_2.2.2)(CF_3SO_3)_3 \cdot CH_3CN \cdot H_2O$. A crystal of sufficient quality suitable for charge-coupled device X-ray analysis was obtained by phase crystallization in a diethyl ether atmosphere. A crystal of this compound was mounted on a glass fiber and then flash-frozen to 100 K (Oxford Cryosystem−Cryostream Cooler). Preliminary examination and intensity data collections were carried out on a KUMA KM4CCD diffractometer[16] using graphite-monochromated Mo Kα radiation (0.710 73 Å). The unit cell parameters were obtained from the positions of 7628 peaks. A total of 57 978 reflections ($3.35° \le \theta \le 28.67°$) was collected. A total of 11 049 unique reflections was used for structural determination. All data were corrected for Lorentz and polarization effects.[17] Absorption corrections based on least-squares fitting against $|F_c| - |F_o|$ differences were also employed,[18] which resulted in transmission factors ranging from 0.298 to 0.432. The space group was chosen from systematic absences and subsequent least-squares refinement. The structure was solved by direct methods (SHELXS97)[19] and refined by full-matrix least squares on F^2 using SHELXL97.[19] Non-hydrogen atoms were refined with anisotropic thermal parameters. The carbon-bound hydrogen atoms were included at calculated positions and refined using a riding model with isotropic-displacement parameters equal to $1.2U_{eq}$ of the attached atom. The H atoms of water molecules were located from difference Fourier maps and refined with restraints. Scattering factors were obtained from the literature.[20] The resultant structure is depicted in Figure 1. The crystal data and some features of the structure refinement are summarized in Table 1; full details have been deposited asSupporting Information.

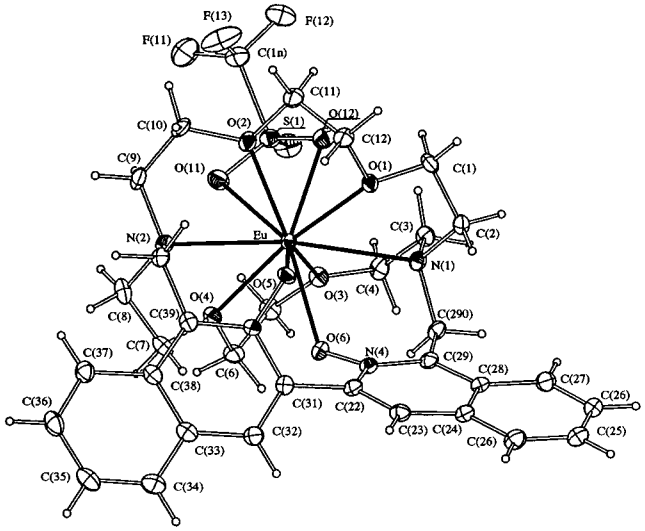

Figure 1. Crystal structure and atomic labels for $(Eu: biqO_2.2.2)(CF_3SO_3)_3 \cdot CH_3CN \cdot H_2O$.

Table 1. Crystallographic Data for $(Eu:biqO_2.2.2)(CF_3SO_3)_3 \cdot CH_3CN \cdot H_2O$

chemical formula	$C_{37}H_{43}EuF_9N_5O_{16}S_3$	Z	8
formula weight	1232.90	ρ_{calcd}, g/cm^3	1.775
crystal system	orthorhombic	μ, mm^{-1}	1.607
space group	*Pbca*	λ, Å	0.710 73
a, Å	12.839(3)	T, K	100.0(5)
b, Å	24.285(5)	R^a	0.0279
c, Å	29.587(6)	$R_w{}^b$	0.0536
V, Å^3	9225(3)		

$^a R_1 = \sum(F_o - F_c)/\sum F_o$. $^b wR_2 = \{\sum[w(F_o^2 - F_c^2)^2]/\sum[w(F_o^2)^2]\}^{1/2}$.

For purposes of discussion we will designate the Eu(III) cryptate with triflate counterions as $Eu\subset 1(tf)_3$. Comparison will be made to previously published results in which the final compound contained 1 equiv of a bromide counterion. This species will be designated as $Eu\subset 1(tf)_2(Br)$. Absorption, emission, and excitation spectra were measured in H_2O, D_2O, CH_3CN (purified by distillation over CaH_2), frozen solution, and the solid state. Solid and frozen solution samples were studied by putting powder samples between quartz slides. The tem-

(9) Lehn, J.-M. In *Supramolecular Photochemistry*; Balzani, V., Ed.; Reidel: Dordrecht, The Netherlands, 1987; pp 29−42.
(10) Pietraszkiewicz, M.; Karpiuk, J.; Pietraszkiewicz, O. *Spectrochim. Acta, Part A* **1998**, *54*, 2229−2236.
(11) Prodi, L.; Maestri, M.; Balzani, V.; Lehn, J.-M.; Roth, C. *Chem. Phys. Lett.* **1991**, *180*, 45−50.
(12) Lehn, J.-M.; Roth, C. O. *Helv. Chim. Acta* **1991**, *74*, 572−578.
(13) Gawryszewska, P. P.; Pietraszkiewicz, M.; Riehl, J. P.; Legendziewicz, J. *J. Alloys Compd.* **2000**, *300−301*, 283−288.
(14) Alpha, B.; Anklam, E.; Deschenaux, R.; Lehn, J.-M.; Pietraszkiewicz, M. *Helv. Chim. Acta* **1988**, *71*, 1042.
(15) Lehn, J.-M.; Pietraszkiewicz, M.; Karpiuk, J. *Helv. Chim. Acta* **1990**, *73*, 106−111.
(16) Kuma Diffraction KM4CCD System Software. *Users Guide*, version 1.161; Kuma Diffraction Spolka Zoo: Wroclaw, Poland, 1195−1999.
(17) Starynowicz, P. COSABS99. *Program for Absorption Correction*; University of Wroclaw: Wroclaw, Poland, 1999.
(18) Sheldrick, G. M. *Acta Crystallogr.* **1990**, *A46*, 467.
(19) Sheldrick, G. M. SHELXL97. *Program for the Refinement of Crystal Structures*; University of Gottingen: Gottingen, Germany, 1997.
(20) Cromer, D. T.; Waber, J. T. In *International Tables for X-ray Crystallography*; Ibers, J. A., Hamilton, W. C., Eds.; Kynoch: Birmingham, England, 1974.

perature of the samples was varied from 4 to 293 K. Absorption measurements were performed using a Cary-Varian 5 spectrophotometer. The emission and excitation spectra at atmospheric pressure were recorded at the University of Wroclaw using a SPECTRAPRO equipped with a 450 W Xe lamp, a liquid-N_2-cooled cryostat, and an Oxford helium flow cryostat. Luminescence and excitation measurements on solutions at elevated pressures were obtained at Michigan Technological University using a NOVA-SWISS high-pressure liquid cell containing three sapphire windows inserted into the sample compartment of a SPEX Fluorolog II spectrofluorimeter as described previously.[21,22] Luminescence decay times were measured on a Jobin-Yvon THR1000 system using a Lambda-Physik 105 excimer laser.

3. Results and Discussion

X-ray Analysis. Single-crystal X-ray diffraction data show that the structure of the compound formed is rhombic with a *Pbca* space group. The unit cell of dimensions $a = 12.839(3)$ Å, $b = 24.285(5)$ Å, and $c = 29.287(6)$ Å and $\alpha = \beta = \gamma = 90°$ consists of eight formula units. The molecular structure of Eu⊂1(tf)$_3$ with the numbering scheme for atoms is displayed in Figure 1. As can be seen in this figure, a surprising result is that the coordination number of Eu(III) in this solid complex is 10. As expected, all of the oxygen and nitrogen atoms of the cryptand are involved in metal-ion coordination. However, two oxygen atoms from one of the triflate counterions are also coordinated. The structure does contain one water molecule and one CH_3CN solvent molecule as outersphere species, in addition to the remaining two $CF_3SO_3^-$ counterions. The inclusion of the triflate counterion in the coordination sphere suggests relatively strong competition of $CF_3SO_3^-$ in the coordination of Eu(III) with water and solvent molecules. This was quite unexpected. As can be seen in Figure 1, $CF_3SO_3^-$ is coordinated in a bidentate manner and is located on the side opposite to the two oxygen atoms of the biqO_2 moiety and between the other two arms of the cryptand. Water molecules and uncoordinated triflate counterions are involved in hydrogen bonding and help to stabilize the overall crystal structure.

Selected bond lengths and selected angles concerning the coordination geometry are given in Table 2. The shortest Eu−O bonds (2.3792 and 2.3872 Å) are associated with the oxygen atoms of the biqO_2 unit. These bond distances are comparable with those found in Eu(bypO_2)$_4$(ClO_4)$_3$ (2,2′-bipyridine-*N*-oxide = bypO_2) which forms a crystal in which Eu(III) has D_2 site symmetry.[23,24] Comparable but somewhat shorter Eu−O bond distances have been reported in the X-ray structure of Eu(bypO_2)$_2$(ClO_4)$_3$·$^3/_2$$CH_3CN$.[25,26] It is worth noting that the Eu(III)−O bonds with the four oxygen atoms of two arms of the cryptand are very similar. There does appear to be a slight lengthening of the Eu−O(3) and Eu−O(2) bonds, which connect to different arms of the cryptand, and a slight shortening of the Eu−O(1) and Eu−O(4) bonds. These bond lengths range from 2.4653 Å for Eu−O(4) to 2.5098 Å for Eu−O(3). This asymmetry must result from the accommodation of the coordinated triflate counterion. The Eu−O(11) and Eu−O(12) bond lengths associated with the coordinated triflate oxygens are longer than the other Eu−O bonds (2.6750 and 2.6498 Å) but are considerably shorter than the Eu−N(1) (2.7907 Å) and Eu−N(2) (2.7566 Å) bonds. The two isoquinoline groups form almost perfect planes. For example, the root mean square (rms) deviation of atoms C(21) to C(29) from perfectly planar is only 0.024. The angle between the two isoquinoline planes is 41.71°. This angle is much less than that seen between the bipyO_2 planes in Nd(bypO_2)$_4^{3+}$, where the angles vary from 57.7 to 65.9°.[27] Obviously, the orientation of these planes is influenced to a large extent by steric constraints imposed by the macrocyclic ring structure. The angle between the isoquinoline planes is similar to that observed for a Eu(III) cryptate containing two bipyridine units and one biqO_2.[28] It should be noted that the size of the cavity containing the Eu(III) ion is not very large; the N(1)−N(2) distance is 5.516(3) Å, and the O(2)−O(3) and O(4)−O(1) distances are 4.639(3) and 4.929(3) Å, respectively.

Table 2. Selected Bond Lengths (Å) and Angles (deg) for (Eu:biqO_2.2.2)(CF_3SO_3)$_3$·CH_3CN·H_2O

Eu−O(6)	2.3792(15)	Eu−O(3)	2.5098(16)
Eu−O(5)	2.3872(16)	Eu−O(12)	2.6498(17)
Eu−O(4)	2.4653(15)	Eu−O(11)	2.6750(17)
Eu−O(1)	2.4814(15)	Eu−N(2)	2.7566(19)
Eu−O(2)	2.4844(16)	Eu−N(1)	2.7907(19)
O(6)−Eu−O(5)	66.48(5)	O(4)−Eu−O(11)	69.25(5)
O(6)−Eu−O(4)	68.70(5)	O(1)−Eu−O(11)	120.63(5)
O(5)−Eu−O(4)	103.39(5)	O(2)−Eu−O(11)	72.74(5)
O(6)−Eu−O(1)	102.14(5)	O(3)−Eu−O(11)	68.97(5)
O(5)−Eu−O(1)	68.54(5)	O(12)−Eu−O(11)	53.07(5)
O(4)−Eu−O(1)	170.09(5)	O(6)−Eu−N(2)	100.89(5)
O(6)−Eu−O(2)	146.90(5)	O(5)−Eu−N(2)	67.91(5)
O(5)−Eu−O(2)	80.49(5)	O(4)−Eu−N(2)	63.91(5)
O(4)−Eu−O(2)	119.67(5)	O(1)−Eu−N(2)	115.93(5)
O(1)−Eu−O(2)	65.80(5)	O(2)−Eu−N(2)	62.62(6)
O(6)−Eu−O(3)	76.67(5)	O(3)−Eu−N(2)	124.44(5)
O(5)−Eu−O(3)	143.04(5)	O(12)−Eu−N(2)	117.45(5)
O(4)−Eu−O(3)	63.90(5)	O(11)−Eu−N(2)	76.09(5)
O(1)−Eu−O(3)	118.80(5)	O(6)−Eu−N(1)	67.95(5)
O(2)−Eu−O(3)	136.42(5)	O(5)−Eu−N(1)	101.12(5)
O(6)−Eu−O(12)	139.73(5)	O(4)−Eu−N(1)	114.80(5)
O(5)−Eu−O(12)	137.93(5)	O(1)−Eu−N(1)	62.94(5)
O(4)−Eu−O(12)	116.44(5)	O(2)−Eu−N(1)	123.47(5)
O(1)−Eu−O(12)	72.87(5)	O(3)−Eu−N(1)	60.44(5)
O(2)−Eu−O(12)	68.78(5)	O(12)−Eu−N(1)	74.85(5)
O(3)−Eu−O(12)	71.91(5)	O(11)−Eu−N(1)	115.83(5)
O(6)−Eu−O(11)	134.10(5)	N(2)−Eu−N(1)	167.31(5)
O(5)−Eu−O(11)	142.15(5)		

The consequences of solvent penetration into the coordination sphere of luminescent lanthanide ions may be very substantial, and therefore, it is useful to examine the details of the penetration of the inner coordination sphere of Eu⊂1 by the $CF_3SO_3^-$ counterion. It appears to have entered the inner coordination sphere of Eu(III) by opening up the slit between the two arms of cryptand approaching from the opposite side to that of the biqO_2 unit. The angles O(4)−Eu−O(11) and O(3)−Eu−O(12) are 69.25(5) and 71.91(5)°, respectively, and the O(11)−Eu−O(2) and O(12)−Eu−O(1) angles are 72.74(5) and 72.87(5)°, respectively. These differences show a slight dislocation of one arm relative to the other because of the presence of the CF_3 moiety. The plane formed by Eu(III) and the two coordinated oxygens from the triflate ion is almost perpendicular [83.27(6)°] to the plane formed by Eu(III) and the two *N*-oxide oxygens. As discussed in more detail below, we have spectroscopic evidence for the penetration of water

(21) Maupin, C. L.; Meskers, S. C. J.; Dekkers, H. P. J. M.; Riehl, J. P. *J. Phys. Chem.* **1998**, *102*, 4450−4455.
(22) Maupin, C. L.; Logue, M. W.; Leifer, L.; Riehl, J. P. *J. Alloys Compd.* **2000**, *300*−*301*, 101−106.
(23) Al-Karaghouli, A. R.; Day, R. O.; Wood, J. S. *Inorg. Chem.* **1978**, *17*, 3702−3706.
(24) Huskowska, E.; Turowska-Tyrk, I.; Legendziewicz, J.; Riehl, J. P. Unpublished work.
(25) Seminara, A.; Rizzarelli, E. *Inorg. Chim. Acta* **1980**, *40*, 249−56.
(26) Lipkowski, J.; Suwinska, K.; Andreeti, G. *Collect. Abstr., XII Eur. Crystallogr. Meet., Moscow, USSR* **1989**, *2*, 272.
(27) Turowska-Tyrk, I.; Huskowska, E.; Legendziewicz, J. Unpublished work.
(28) Paul-Roth, C. O.; Lehn, J.-M.; Guilhem, J.; Pascard, C. *Helv. Chim. Acta* **1995**, *78*, 1895−1902.

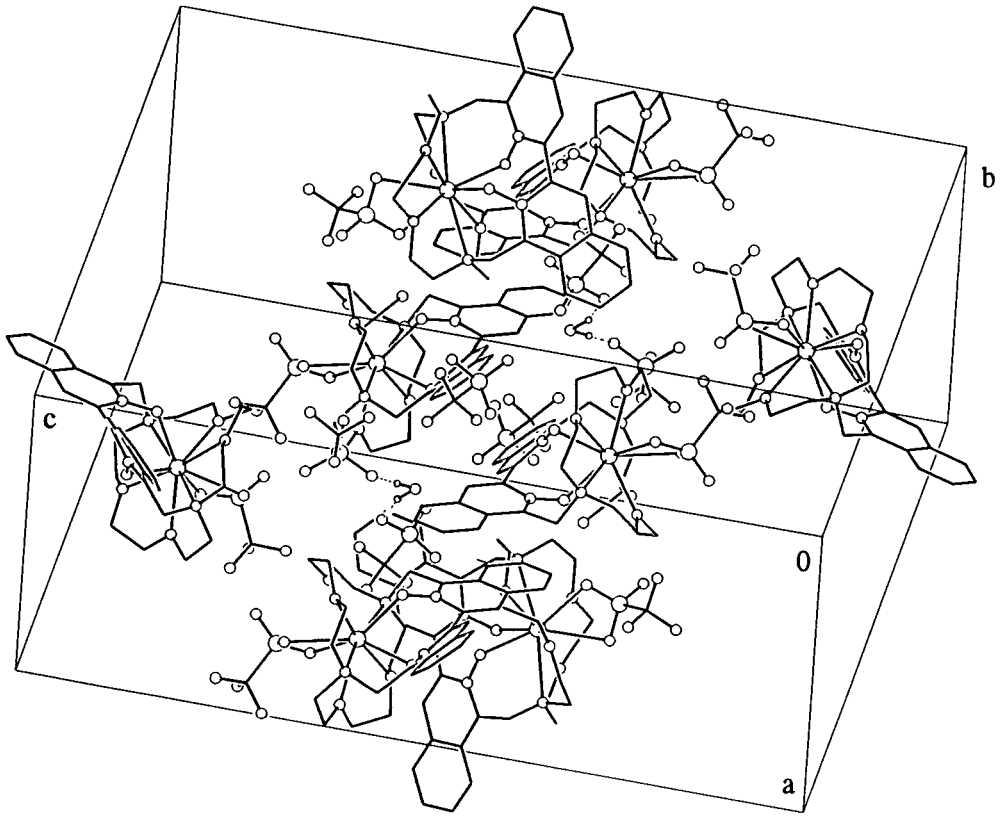

Figure 2. Packing diagram for crystalline (Eu:biqO_2.2.2)$(CF_3SO_3)_3$·CH_3CN·H_2O.

into the first coordination sphere in solution, and this structural data suggests the most likely mechanism for this effect.

The packing of the crystal lattice is presented in Figure 2. As required by symmetry, the unit cell contains enantiomeric complexes. Attempts to measure circularly polarized luminescence by using circularly polarized excitation[29] to generate a nonracemic excited (emitting) state from a racemic ground state in solution were not successful. These could be due to either equilibration of enantiomers on a time scale faster than that of the luminescence, a solution structure that is not chiral, or other reasons associated with the chirality of the spectroscopic transitions used for the measurement. Note also the symmetric distribution of CH_3CN and the uncoordinated triflate counterions in the unit cell.

Spectroscopic Results. The absorption spectra of Eu⊂1$(tf)_3$ in the UV region in the solid state, as well as dissolved in H_2O and CH_3CN, are presented in Figure 3. These spectra were all recorded at room temperature. It should be noted that the absorption spectrum of the complex dissolved in CH_3CN is unchanged after several days, indicating that the complex is reasonably stable under these conditions. As can be seen in this figure, the absorption spectrum in this region exhibits several transitions at 268, 335, and 355 nm associated with $\pi \rightarrow \pi^*$ transitions of the heteroaromatic ligand. The noise at low wavelengths for the solid spectrum is due to the difficult nature of these measurements. The absorption spectrum in solution is virtually identical to that reported previously for Eu⊂1$(tf)_2$(Br). Under these conditions of concentration and temperature, there is no evidence for ligand-to-metal charge-transfer transitions (LMCT) or intraconfigurational f → f absorption transitions, which are expected to be very weak.

In Figures 4 and 5, we plot high-resolution luminescence

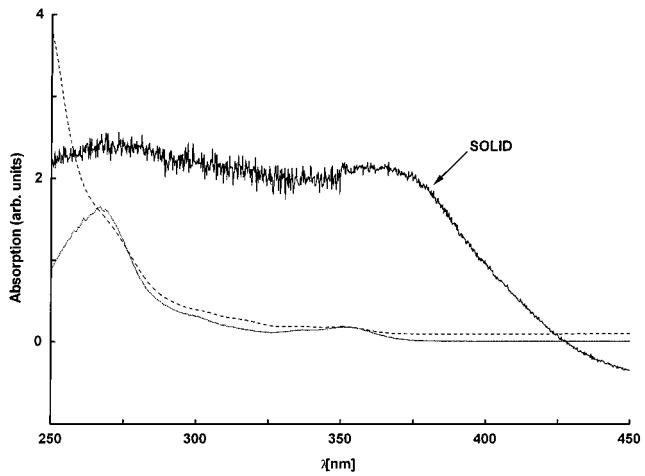

Figure 3. Absorption spectra for solid (Eu: biqO_2.2.2)$(CF_3SO_3)_3$·CH_3CN·H_2O and solutions of (Eu: biqO_2.2.2)$^{3+}$ dissolved in water (dotted line) and acetonitrile (dashed line). All spectra were recorded at room temperature.

spectra in the region corresponding to the $^5D_0 \rightarrow {}^7F_0$, $^7F_1$, and $^7F_2$ transitions of Eu(III) in Eu⊂1. In Figure 4, we compare results for a quickly frozen solid sample of Eu⊂1$(tf)_3$ (A) and similar measurements made several days (B) and several weeks (C) later on the same sample. Of particular note is the large intensity of the $^5D_0 \rightarrow {}^7F_0$ peak at 579.20 nm and the observation that additional peaks in the spectrum appear as the sample is allowed to stand. The appearance of additional peaks in the $^5D_0 \rightarrow {}^7F_0$ region of the spectrum is indicative of the formation of new species, and because it is almost impossible to exclude small amounts of water in preparing these samples for spectroscopic measurements, the most likely explanation of the new peak is the either partial or complete replacement of the coordinated triflate ion with a water molecule. These types of

(29) Hilmes, G. L.; Riehl, J. P. *J. Phys. Chem.* **1983**, *87*, 3300−04.

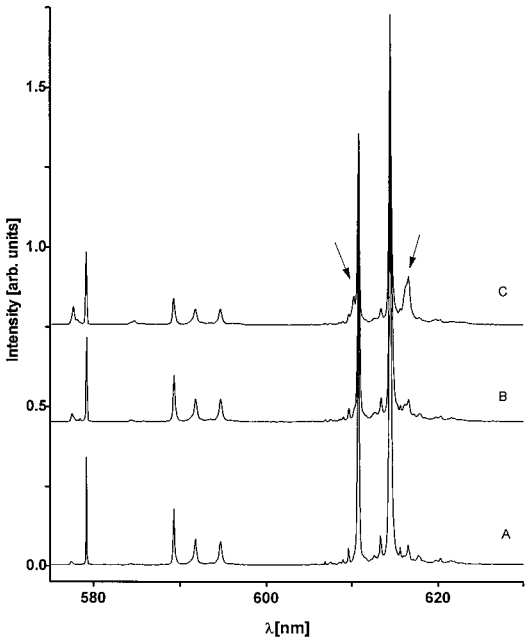

Figure 4. Luminescence spectrum of Eu⊂1(tf)$_3$ at 77 K (A) immediately after being frozen, (B) several hours later, and (C) several days later.

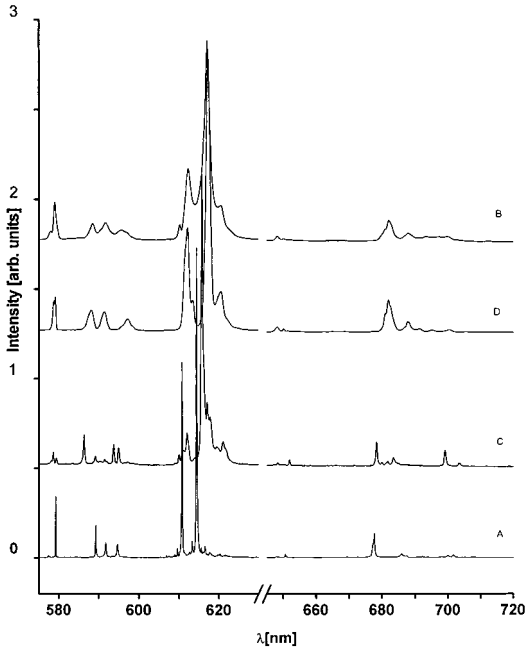

Figure 5. Luminescence spectra of solid Eu⊂1(tf)$_3$ (A) and solid Eu⊂1(tf)$_2$(Br) (C) at 77 K and frozen CH_3CN solutions of Eu⊂1(tf)$_3$ (B) and solid Eu⊂1(tf)$_2$(Br) (D).

changes are more obvious in the results presented in Figure 5, where we compare results for solid Eu⊂1(tf)$_3$ and Eu⊂1(tf)$_2$(Br) and solutions of these two cryptate solids dissolved in CH_3CN at 77 K. As one can see, changes in the counterions lead to noticeable modifications of the luminescence spectrum.

Considering the manner in which the cryptate has opened up to allow coordination to the triflate ion in the crystal structure, it is not surprising that the first coordination sphere can accommodate other species. This is what we conclude from the appearance of two peaks in the region of the $^5D_0 \rightarrow {}^7F_0$ transition at 77 K. This should also result in additional components in the other europium transitions. As can be seen in Figure 4, the $^5D_0 \rightarrow {}^7F_2$ transition (612−620 nm) contains two strong lines

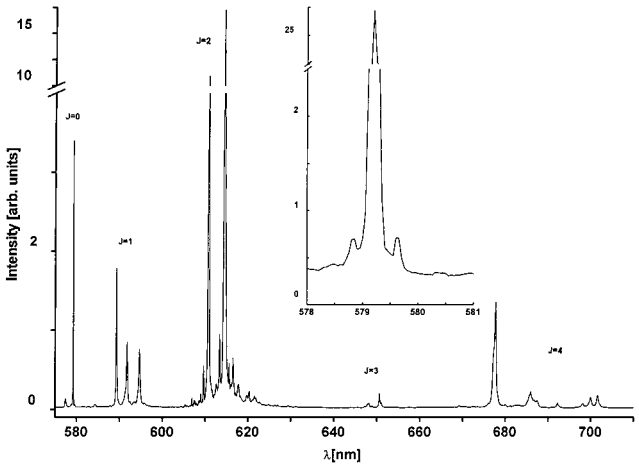

Figure 6. Luminescence spectrum for a quickly frozen sample of solid Eu⊂1(tf)$_3$. The inset in this figure is an enlargement of the $^5D_0 \rightarrow {}^7F_0$ transition.

which must be associated with pure electronic crystal field transitions for the major species present and a number of smaller peaks which may be due to electronic components of the minor species or a result of strong electron−phonon coupling in this system. Among the weak components of the $^5D_0 \rightarrow {}^7F_2$ transition, the two peaks indicated by arrows on curve C in Figure 4 increase in intensity in line with the increase in intensity of the $^5D_0 \rightarrow {}^7F_0$ component at 577.45 nm, so these can be associated with the modified form of the cryptand. There is no evidence for additional peaks for the magnetic dipole transition $^5D_0 \rightarrow {}^7F_1$ (588−596 nm). This transition is very weak and relatively insensitive to the Eu(III) environment, and it may be that the additional peaks overlap with the three components of the major species.

The explanation that the changes observed as a function of time are due to solvent penetration and replacement of the counterion in the inner coordination sphere is further demonstrated by the spectra of Eu⊂1(tf)$_3$ and Eu⊂1(tf)$_2$(Br) presented in Figure 5. Although the spectra of the solid cryptates (A and C) are very complex and different for these two species, dissolving the solids in CH_3CN leads to almost the same spectra (B and D). Some subtle differences still appear in the luminescence spectra. This is most easily seen in the $^5D_0 \rightarrow {}^7F_2$ spectral region for samples B and D, but these are most likely due to differences in sample preparation and handling.

In Figure 6, we plot the luminescence spectrum for the quickly frozen Eu⊂1(tf)$_3$ solid sample on an enlarged vertical scale to highlight the weak components in the spectrum. The insert in this figure is a further enlargement of the $^5D_0 \rightarrow {}^7F_0$ transition showing Stokes and anti-Stokes vibronic components on respective sides of the much stronger pure electronic transition. A much more complex vibronic structure is seen in the $^5D_0 \rightarrow {}^7F_2$ transition. The superposition of the infrared spectrum onto the 0 phonon lines shows strong electron−phonon coupling, mainly associated with internal ligand modes. The strongest coupling was observed with the N−O vibrations associated with the coordinated biqO_2 group. The vibronic components were assigned on the basis of the IR spectrum and are listed in Table 3. A detailed analysis of the vibronic components and a comparison with IR and Raman measurements will be the subject of a forthcoming paper.

In the structure presented in Figure 1, the Eu(III) ion is located in a site of C_1 symmetry because of the incorporation of the triflate anion. The coordination polyhedron (CN = 10) can be described as a bicapped dodecahedron, which can possess either

Table 3. Vibronic Components for Single Crystals of (Eu: $biqO_2.2.2)(CF_3SO_3)\cdot CH_3CN\cdot H_2O$

transition	energy [cm^{-1}]	ΔE
$^5D_0 \rightarrow {}^7F_0$	17 265	
	17 202	63
	17 012	253
	16 519	746
	16 477	788
	16 462	803
	16 433	833
	16 420	845
	16 324	941
	16 244	1021
	16 189	1076
	16 137	1128
	16 091	1174
	16 054	1211
	16 051	1214
	16 002	1263
	15 949	1316
	15 888	1377

D_2 or C_{2v} symmetry. D_2 symmetry was excluded because of the strong intensity of the $^5D_0 \rightarrow {}^7F_0$ transition, which is forbidden for this symmetry. Because the bound triflate oxygens are aligned almost perpendicular to the bound *N*-oxide oxygens, the Eu(III) environment is very close to C_2 symmetry. However, in the analysis of electronic transitions for lanthanide(III) ions, it is often the case that a reasonable analysis can be derived by the consideration of only the coordinated atoms. Under this assumption the site symmetry may be approximated by C_{2v} symmetry. The electronic selection rules for the Eu(III) transitions in C_{2v} symmetry are presented in Table 4. We also present in this table the number of electronic transitions predicted and the number that are observed. It should be noted that we did not observe any lines associated with transitions from the $^5D_1$ state, in contrast to the results of Blasse et al.[30] in the low-temperature spectra of a Eu(III) cryptate with three bipyridine units. As can be seen from the data given in Table 4, the luminescence results match the predictions based upon C_{2v} selection rules fairly well. The major discrepancy is in the number of lines predicted for the $^5D_0 \rightarrow {}^7F_2$ transition where a total of four lines are predicted and only two strong lines ($2A_1$) are observed. As described above, it is somewhat difficult to sort out vibronic transitions from weak electronic ones, and the situation is further complicated by the presence of a second structure, presumably due to the incorporation of a water molecule in the coordination sphere. It is certainly possible that there may be overlap of transitions, or it could be that some of the components are weak.

To probe the excited-state energetics of this system, we have measured the fluorescence decay times and quantum yields of the solid $Eu\subset 1(tf)_3$ and the complex dissolved in H_2O, D_2O, and CH_3CN. The results are presented in Table 5. The measurement of the lifetimes in H_2O and D_2O solutions allows one to estimate the number of Eu(III)-bound water molecules, *n*, using the following equation derived by Horrocks and Sudnick[31]

$$n = 1.05[\tau(H_2O)^{-1} - \tau(D_2O)^{-1}] \quad (1)$$

where the lifetimes are measured at room temperature and are entered in milliseconds. The substitution of the measured lifetimes into this equation yields a value for *n* of 1.36. The accuracy of this method is assumed to be ± 0.5, so this result is consistent with the presence of approximately one molecule of water in the first coordination sphere as a result of exchange with the coordinated triflate anion as suggested by the crystal structure.

It is also possible to estimate the other temperature-dependent and temperature-independent parts of the nonradiative decay constants in the manner of Prodi et al.[11] In this analysis, the overall decay constant, *k*, is expressed as

$$k = 1/\tau = k_r + k_{nr}(T) + k_{nr}(\text{OH}) + k_{nr}(\text{other vibrations}) \quad (2)$$

where k_r is the radiative decay constant and $k_{nr}(T)$ is the temperature-dependent nonradiative decay constant, and it is assumed that the most important mechanism for temperature-independent nonradiative relaxation is through OH oscillators. Under the additional assumptions that vibrations other than OH (including OD) can be neglected and that $k_{nr}(77\ \text{K})$ is also not important, one can derive the expressions

$$k_r = [\tau(D_2O)_{77K}]^{-1} \quad (3)$$

and

$$k_{nr}(T) = [\tau(D_2O)_{300K}]^{-1} - [\tau(D_2O)_{77K}]^{-1} \quad (4)$$

Comparing the results we obtain to those reported previously, we see that the radiative decay rate ($1243\ s^{-1}$) is significantly larger than that which results from related cryptates involving bipyridine units.[11] This difference probably reflects the assumption implied by eq 3 that there are no competing nonradiative deactivation processes at 77 K. The inclusion of the triflate anion in the crystal structure suggests that this assumption might not be valid for this system. The temperature-dependent nonradiative decay rate ($463\ s^{-1}$) is quite similar to previously obtained values. For example, Prodi et al.[11] report a value of $600\ s^{-1}$ for $k_{nr}(T)$ for a Eu(III) cryptate containing two bpy units and one $biqO_2$ group. This is consistent with the interpretation that this term reflects thermally activated back energy transfer from Eu(III) orbitals to ligand triplet states and, perhaps, short-lived LMCT states.

No ligand phosphorescence could be detected from $Eu\subset 1$, and no luminescence could be detected from $Tb\subset 1$ at 4 and 300 K. The latter result is consistent with the triplet level of $biqO_2$ being situated near or below the $^5D_4$ excited-state level of Tb(IIII) which is located at approximately 20 500 cm^{-1}. Ligand phosphorescence was observed from $Gd\subset 1$ at approximately 18 018 cm^{-1}. The $^5D_0$ of Eu(III) is situated at approximately 17 265 cm^{-1}. Thus, the energy gap between the ligand $^3\pi\pi^*$ state and the $^5D_0$ level is 763 cm^{-1}. This is significantly lower than that (2100 cm^{-1}) determined from the fluorescence and phosphorescence data of model complexes.[11] The strong temperature dependence of the luminescence lifetime reflected in $k_{nr}(T)$ suggests that the LMCT states of $Eu\subset 1(tf)_3$ might also take part in nonradiative deactivation of excited Eu(III), because they are most probably located at comparable energies.[32] The relatively short decay times and strong temperature dependence, observed for the solid and the CH_3CN solution, suggest that other quenching mechanisms should be considered for these systems.

(30) Blasse, G.; Dirksen, G. J.; Van der Voort, D.; Sabbatini, N.; Perathoner, S.; Lehn, J.-M.; Alpha, B. *Chem. Phys. Lett.* **1988**, *146*, 347−351.
(31) Horrocks, W. DeW.; Sudnick, D. R. *Acc. Chem. Res.* **1981**, *14*, 384.
(32) Sabbatini, N.; Guardigli, M.; Leh, J.-M. *Coord. Chem. Rev.* **1993**, *123*, 201−228.

Table 4. Electronic Selection Rules for Eu(III) Transition in C_{2v} Symmetry and the Number of Electronic Transitions Predicted and Observed (ED = electric dipole; MD = magnetic dipole)

	$J=0$			$J=1$			$J=2$			$J=3$			$J=4$		
		ED	MD		ED	MD		ED	MD		ED	MD		ED	MD
C_2v	A_1	+	−	A_2	−	+	$2A_1$	+	−	A_1	+	−	$3A_1$	+	−
				B_1	+	+	A_2	−	+	$2A_2$	−	+	$2A_2$	−	+
				B_2	+	+	B_1	+	+	$2B_1$	+	+	$2B_1$	+	+
							B_2	+	+	$2B_2$	+	+	$2B_2$	+	+
predicted		1			3			4 + 1 weak			5 + 2 weak			7 + 2 weak	
observed		1			3			2 + 2 weak			6			7	

Table 5. Luminescence Decay Data for Eu⊂1(tf)$_3$ Cryptate in Solids and Solutions at 300 and 77 K [Lifetimes in milliseconds; Rate Constants in s^{-1}]

compounds	E_{0-0}	τ_{77K}	$\tau(D_2O)_{77K}$	τ_{300K}	$\tau(D_2O)_{300K}$	k_r	$k_{r,nr}(OH)^a$	$k_{nr}(T)^b$	$\sum k^c$	$n(H_2O)$
Eu⊂1(tf)$_3$ solid	17 265	0.611		0.059						
Eu⊂1(tf)$_3$ in H_2O		0.633	0.804	0.336	0.586	1243	1270	463	2976	1.36
Eu⊂1(tf)$_3$ in CH_3CN		0.4119		0.0264						

[a] Defined as $1/\tau(H_2O)_{300K} - 1/\tau(D_2O)_{300K}$. [b] Calculated from eq 4. [c] Calculated from eq 2.

The rational design of lanthanide-based fluoroimmunoassay agents requires an understanding of the energetics and dynamics of excited-state ligand−lanthanide interactions beyond what is currently available. The results given above do yield important and relevant information about the overall rate constants for the various processes; however, the analysis is based upon a model involving several simplifying assumptions. One additional way in which the subtle population and depopulation kinetics of lanthanide emitting states may be probed is through the application of high pressure. Increased pressure on solution complexes may cause structural changes associated with more compact equilibrium structures,[33] particularly changes toward lower charged species because of solvent electrostriction,[34] and it may impact electronic structure. Previously we have shown that the effect of high pressure (up to 3 kbar) on k_r for several multidentate and macrocyclic aqueous Eu(III) complexes is very weak.[22,33] This is not surprising because the f orbitals do not extend very far from the atomic core. However, the effect on ligand orbitals could be significant. For these reasons, we expect that the principal electronic effect of increased liquid pressure will be in the energy-transfer processes between the ligand triplet state and the Eu(III) excited state and, perhaps, in the energy back transfer.

In Figure 7, we show the results of increased pressure on the luminescence from solutions of Eu⊂1 at room temperature. These measurements were taken on a SPEX Fluorolog instrument that has been adapted to accommodate the high-pressure liquid cell. The resolution of the instrument (4 nm) band-pass was significantly less than the high-resolution measurements given in Figures 4−6. As can be seen, the luminescence intensity increases with pressure, and only very small crystal field splitting differences are seen, that may be associated with slight twisting or other minor distortions of the cryptate substructure. These are most noticeable in the higher wavelength band of the hypersensitive $^5D_0 \rightarrow {}^7F_2$ transition. The effect of increased pressure is more evident in the excitation spectra presented in Figure 8. The total luminescence intensity increases by approximately 25% when the pressure is increased to 3 kbar. These results show that there is little change in the coordination of Eu(III) in the cryptand but a very substantial increase in the population of the $^5D_0$ state because of either an increase in the energy transfer from the ligand triplet state or a decrease in deactivation by back transfer. As a first approximation, a small decrease in distance from the ligand to the metal ion would be expected to increase both forward and reverse energy transfer, although not necessarily equally. More interestingly, increased pressure is known to have a pronounced effect on the energy of ligand π orbitals, so the effect that we observe may be due

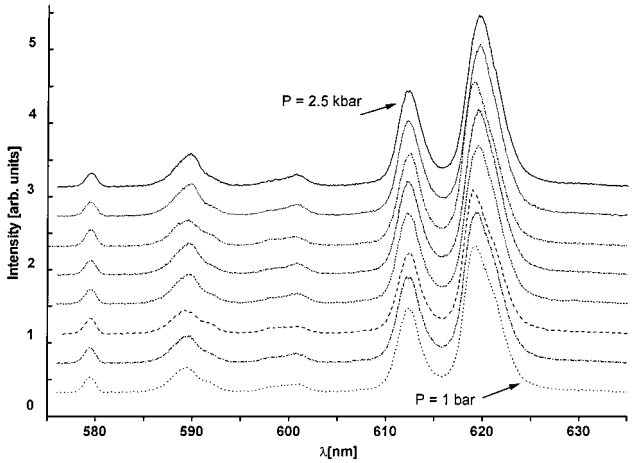

Figure 7. Emission spectra of aqueous solutions of Eu⊂1 under conditions of high liquid pressure. The individual curves represent regular pressure increases from 1 bar to 3 kbar.

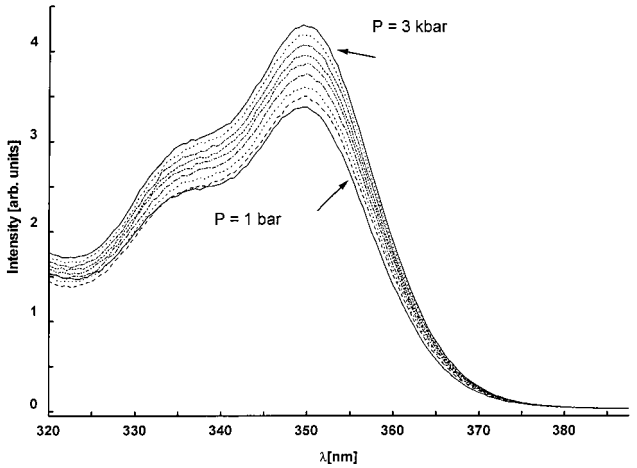

Figure 8. Excitation spectra of aqueous solutions of Eu⊂1 under conditions of high liquid pressure. The various curves represent systematic increases of pressure from 1 bar to 3 kbar.

(33) Mondry, A.; Maupin, C. L.; Leifer, L.; Riehl, J. P. Unpublished work.
(34) van Eldik, R.; Asano, T.; Le Noble, W. J. *Chem. Rev.* **1989**, *89*, 549−688.

to changes in metal−ligand orbital overlap. We are currently designing experiments to probe these types of interactions.

Acknowledgment is made to the National Science Foundation—Division of International Programs (INT-9811606) and the KBN Polish Committee for Scientific Research for partial support of this work. The authors also thank Dr. K. Maruszewski for luminescence decay measurements.

IC0004683